Inhibition of protein arginine methyltransferase 6 activates interferon signaling and induces the apoptosis of endometrial cancer cells via histone modification

FUTABA INOUE[1], KENBUN SONE[1], KOHEI KUMEGAWA[2], RYUTA HACHIJO[1], ERI SUZUKI[1], SAKI TANIMOTO[1], NATSUMI TSUBOYAMA[1], KOSUKE KATO[1], YUSUKE TOYOHARA[1], YU TAKAHASHI[1], MISAKO KUSAKABE[1], ASAKO KUKITA[1], HARUNORI HONJOH[1], AKIRA NISHIJIMA[1], AYUMI TAGUCHI[1], YUICHIRO MIYAMOTO[1], MICHIHIRO TANIKAWA[1], TAKAYUKI IRIYAMA[1], MAYUYO MORI[1], OSAMU WADA-HIRAIKE[1], KATSUTOSHI ODA[3], HIROMU SUZUKI[4], REO MARUYAMA[2,5] and YUTAKA OSUGA[1]

[1]Department of Obstetrics and Gynecology, Graduate School of Medicine, The University of Tokyo, Tokyo 113-8655; [2]Cancer Cell Diversity Project, NEXT-Ganken Program, Japanese Foundation for Cancer Research, Tokyo 135-8550; [3]Division of Integrative Genomics, Graduate School of Medicine, The University of Tokyo, Tokyo 113-8655; [4]Department of Molecular Biology, Sapporo Medical University School of Medicine, Sapporo 060-8556; [5]Project for Cancer Epigenomics, Cancer Institute, Japanese Foundation for Cancer Research, Tokyo 135-8550, Japan

Received December 29, 2022; Accepted October 10, 2023

DOI: 10.3892/ijo.2024.5620

Abstract. Histone modification, a major epigenetic mechanism regulating gene expression through chromatin remodeling, introduces dynamic changes in chromatin architecture. Protein arginine methyltransferase 6 (PRMT6) is overexpressed in various types of cancer, including prostate, lung and endometrial cancer (EC). Epigenome regulates the expression of endogenous retrovirus (ERV), which activates interferon signaling related to cancer. The antitumor effects of PRMT6 inhibition and the role of PRMT6 in EC were investigated, using epigenome multi-omics analysis, including an assay for chromatin immunoprecipitation sequencing (ChIP-seq) and RNA sequencing (RNA-seq). The expression of PRMT6 in EC was analyzed using reverse transcription-quantitative polymerase chain reaction (RT-qPCR) and immunohistochemistry (IHC). The prognostic impact of PRMT6 expression was evaluated using IHC. The effects of PRMT6-knockdown (KD) were investigated using cell viability and apoptosis assays, as well as its effects on the epigenome, using ChIP-seq of H3K27ac antibodies and RNA-seq. Finally, the downstream targets identified by multi-omics analysis were evaluated. PRMT6 was overexpressed in EC and associated with a poor prognosis. PRMT6-KD induced histone hypomethylation, while suppressing cell growth and apoptosis. ChIP-seq revealed that PRMT6 regulated genomic regions related to interferons and apoptosis through histone modifications. The RNA-seq data demonstrated altered interferon-related pathways and increased expression of tumor suppressor genes, including NK6 homeobox 1 and phosphoinositide-3-kinase regulatory subunit 1, following PRMT6-KD. RT-qPCR revealed that eight ERV genes which activated interferon signaling were upregulated by PRMT6-KD. The data of the present study suggested that PRMT6 inhibition induced apoptosis through interferon signaling activated by ERV. PRMT6 regulated tumor suppressor genes and may be a novel therapeutic target, to the best of our knowledge, in EC.

Correspondence to: Dr Kenbun Sone, Department of Obstetrics and Gynecology, Graduate School of Medicine, The University of Tokyo, 7-3-1 Hongo Bunkyo-ku, Tokyo 113-8655, Japan
E-mail: ksone5274@gmail.com

Abbreviations: DAVID, Database for Annotation Visualization and Integrated Discovery; EC, endometrial cancer; PRMT, protein arginine methyltransferase; RNA-seq, RNA sequencing; IS, intensity score; PS, proportion score; PI, propidium iodide; TS, total score; FACS, fluorescence-activated cell sorting; GO, Gene Ontology; GREAT, Genomic Regions Enrichment of Annotations Tool; OS, overall survival; DFS, disease-free survival; NFATC1, nuclear factor of activated T-cells 1; EMT, epithelial-mesenchymal transition; SD, standard deviation

Key words: histone arginine methyltransferase; endometrial cancer, PRMT6, apoptosis, interferon

Introduction

Endometrial cancer (EC) is the most commonly occurring gynecological malignancy; the standard treatment includes surgical interventions, followed by the administration of anti-cancer therapeutics for high-risk patients (1,2). Patient prognosis is good in the early stages; however, advanced or recurrent disease is refractory (3). The use of a molecular targeting drugs for the treatment of EC was approved for the first time last year. Thus, the number of available molecular target therapeutics for EC therapy is limited, in comparison with ovarian cancer (3).

Regardless of the advances in cancer genome research and the establishment of thorough databases such as The Cancer Genome Atlas (TCGA), cancer treatment and therapy has yet to be fully elucidated and overcome. Recently, it has been reported that both genomic and epigenomic aberrations are critical in carcinogenesis (4). The molecular mechanisms of the cancer epigenome are mostly divided into DNA methylation and histone modification. DNA methylation only regulates a single gene by methylating a single base, whereas histone modification regulates downstream genes in a multilayered manner, through acetylation, methylation and the phosphorylation of the histone proteins with histone modifying enzymes (5). DNA forms nucleosomes when wrapped around histone proteins; histone modifications regulate transcription by regulating the tightly packed (heterochromatin) and relaxed lightly packed (euchromatin) forms of DNA (6).

Among the histone modifications, histone methylation is carried out by histone methyltransferases and demethylases (7). The histone methylation sites are the lysine and arginine groups of amino acids and the enzymes mediating histone methylation are lysine methyltransferases and arginine methyltransferases. It has been demonstrated that increased expression levels of histone methyltransferases are involved in carcinogenesis and cancer progression (8,9). For example, the lysine histone methyltransferase SUV39H2 has been shown to be highly expressed in lung cancer and SUV39H2 knockdown (KD) increases sensitivity to radiation and chemotherapy (10). In gynecological cancers, a histone lysine methyltransferase, enhancer of zeste homolog 2 (EZH2) was defined as a therapeutic target in EC (11), and Wolf-Hirschhorn syndrome candidate gene-1, Su(var)3-9, enhancer of zeste, trithorax (SET) domain-containing protein 8, and SET and myeloid, nervy, and DEAF-1 (MYND) domain containing 2 were highly expressed in ovarian cancer, with their inhibition attenuating cell proliferation (12-15). Arginine methyltransferase is named as a protein methyltransferase (PRMT) due to its ability to methylate other proteins and not solely histones (16,17). As expected, PRMT and lysine methyltransferase are therapeutic targets for the treatment of various types of cancer, including breast, prostate, lung and blood cancer (18). In a previous study by the authors, it was reported that the expression of PRMT4 [also known as coactivator-associated arginine methyltransferase 1 (CARM1)] was increased in EC, and treatment with a selective inhibitor of CARM1 resulted in the apoptosis-induced suppression of cell proliferation in EC cell lines (19).

PRMT6 is a member of the PRMT group and is highly expressed in various types of cancer, including breast, prostate and lung cancer (20-22) and is involved in cancer-related mechanisms. The histone modification of PRMT6 has been reported to asymmetrically dimethylate the histone H3R2 (H3R2me2a) and it has been reported that H3K27 acetylation (H3K27ac) and H3K4 histone trimethylation (H3K4me3) are affected through the methylation of H3R2 (23). Jiang *et al* (24) reported that the expression of PRMT6 increased in EC, negatively correlated with prognosis, and was associated with cell proliferation in EC cells. However, the mechanism of PRMT6-mediated histone modification in EC remains largely unknown.

Therefore, in the present study, the expression of PRMT6 in EC was investigated, by using clinical specimens from the University of Tokyo Hospital. A KD experiment was performed, in order to examine the cell proliferation mechanism of PRMT6. In addition, chromatin immunoprecipitation sequencing (ChIP-seq) was performed, in order to investigate the genes regulated by PRMT6 via histone modification.

Materials and methods

Clinical samples. EC tissue (n=55) and normal endometrial tissue (n=20) were collected from patients who underwent surgery at the University of Tokyo Hospital between 2010 and 2021. The list of patients is presented in Table SI and written informed consent was acquired from all patients. The median age was 51 years (range, 31-80 years). The samples from patients No. 1 to No. 52, N1 to N4, and N17 to N20 were used for mRNA extraction, and the thin section samples were prepared from patients No. 1 to No. 55 and N5 to N16. Clinical samples used in additional experiments are highlighted in bold in Table SI. The present study was approved by The Human Genome, Gene Analysis Research Ethics Committee of the University of Tokyo (Approval no. G0683-22).

Cell lines and cell culture. A total of six EC cell lines (HEC1B, HEC50B, HEC265, Ishikawa, HEC151A and HEC116) were used in the present study. All cell lines were cultured in Eagle's minimal essential medium (FUJIFILM Wako Pure Chemical Corporation) supplemented with 10% heat-inactivated fetal bovine serum (Thermo Fisher Scientific, Inc.) in a humidified incubator containing 5% CO_2 at 37˚C. All cell lines were not passaged >15 times.

Small interfering RNA (siRNA) transfection. siRNA transfection was performed as previously described (19). Briefly, siRNAs were transfected at 37˚C for 3.5 h using Lipofectamine RNA interference (RNAi)MAX Transfection Reagent (Thermo Fisher Scientific, Inc.), and the final concentration of siRNAs was 100 nM. PRMT6 siRNAs were as follows: siPRMT6#1 sense, 5'-CGGAACAGGUGGAUGCCAU-3'; siPRMT6#1 antisense, 5'-AUGGCAUCCACCUGUUCCG-3'; siPRMT6#2 sense, 5'-ACAGCAUACCUAAGAAACUCAGAAG-3'; siPRMT6#2 antisense, 5'-CUUCUGAGUUUCUUAGGUAUGCUGU-3' (MilliporeSigma). MISSION siRNA Universal Negative Control #1 (siNC) was used as a negative control (Merck KGaA). RNA extraction for reverse transcription-quantitative polymerase chain reaction (RT-qPCR) was performed 72 h following siRNA transfection, and cell viability assay, cell cycle analysis, apoptosis assay and protein extraction for western blotting were performed 96 h following siRNA transfection.

RNA extraction and RT-qPCR. RNA extraction and RT-qPCR were performed according to a previously described procedure (19). Briefly, total RNA was extracted from the cells using the RNeasy Mini kit (Qiagen, Inc.). Reverse transcription was performed using ReverTra Ace qPCR Master Mix with gDNA Remover (Toyobo Co., Ltd.), and single-strand complementary DNA was synthesized. RT-qPCR was carried out using a One-Step SYBR Prime Script RT-PCR kit (Takara Bio, Inc.) on a Light Cycler instrument (Roche Diagnostics) and a QuantStudio instrument (Thermo Fisher Scientific, Inc.). The Thermocycling conditions were as follows: Initial

denaturation step at 98˚C for 2 min, followed by 45 cycles at 98˚C for 10 sec, 60˚C for 10 sec and 68˚C for 30 sec. β-actin was used as a reference gene, and relative gene expression was analyzed using the $2^{-\Delta\Delta Cq}$ method (25). The primer sequences are included in Table SII. The primers for the genes of endogenous retrovirus (ERV) were also designed for the same sequence as previously reported, which was confirmed in the gEVE database (http://geve.med.u-tokai.ac.jp) for the recognition of ERVs (26).

Immunohistochemistry (IHC). Clinical tissues were fixed with 20% neutral buffered formalin at room temperature. The formalin fixation time was usually within 24 h. Formalin-fixed paraffin-embedded sections (thickness, 4-μm) were deparaffined and antigen retrieval was performed with a citric acid buffer (Target Retrieval Solution Citrate, pH6, 10X; Agilent Technologies, Inc.) using an autoclave. Subsequently, the blocking of endogenous peroxidase was performed using 200 μl/section of Dako REAL Peroxidase-Blocking Solution (Agilent Technologies, Inc.) at 25˚C for 10 min. Anti-PRMT6 antibody (1:2,000; cat. no. 15395-1-AP; Proteintech Group, Inc.) was applied as the primary antibody and incubated overnight at 4˚C. The following day, secondary antibody reaction and detection were performed using Dako REAL EnVision Detection System, Peroxidase/DAB, rabbit/mouse, and horseradish peroxidase (HRP; Agilent Technologies, Inc.). Counterstaining was performed with Meyer's hematoxylin solution (0.1% hematoxylin, FUJIFILM WAKO, Tokyo, Japan) at 25˚C for 2 min and dehydrated with ethanol and xylene. The immunostained sections were observed using a biological microscope (BX50F4; Olympus Corporation). The score of PRMT6 expression was calculated by the proportion of stained positive cells [proportion score (PS)] and the intensity of staining [intensity score (IS)], which are calculated as follows: Total score (TS)=PS+IS. PS score 0, 0%; score 1, 1-20%; score 2, 21-40%; score 3, 41-60%; score 4, 61-80%; score 5, >81%. IS score 0, background; score 1, weak staining; score 2, moderate staining; score 3, strong staining. Samples with a score of 0-5 were designated as the PRMT6-low group and those with scores of 6-8 as the PRMT6-high group. The results were recorded by two independent observers, and the average score was calculated.

Cell viability assay. The cell viability assay was performed previously demonstrated (19) and was assessed using the Cell Counting Kit-8 (CCK-8; Dojindo Laboratories, Inc.). The EC cells (HEC1B, HEC50B, HEC265, Ishikawa, HEC151A and HEC116) were transfected with siRNAs were incubated at 37˚C for 96 h. CCK-8 solution (10% amount of medium) was added to each well and incubated at 37˚C for 2 h. The absorbance of the solution was measured at 450 nm using a Synergy LX multimode microplate reader (BioTek Instruments, Inc.).

Cell cycle analysis. The cell cycle analysis was performed as previously described (19). In brief, EC cells were transfected with siRNAs as described earlier and incubated at 37˚C for 96 h. The cells were harvested with trypsin and fixed with 70% ethanol at 4˚C overnight and stained using propidium iodide (MilliporeSigma) at 4˚C for 15 min. The cell cycle analysis was evaluated using fluorescence-activated cell sorting (FACS) on a BD FACSCalibur HG Flow Cytometer Instrument (BD Biosciences) and Cell Quest Pro software version 3.1 (BD Biosciences). The data were calculated using FlowJo software version 16 (FlowJo LLC).

Apoptosis assay. The apoptosis assay was carried out according to a previously described protocol (19). Briefly, the EC cells were transfected with siRNAs as previously described and incubated at 37˚C for 96 h. The cells were harvested using trypsin and stained with the Fluorescein isothiocyanate (FITC) Annexin V Apoptosis Detection Kit II (BD Biosciences) at 25˚C for 15 min. The cells were evaluated using FACS on a BD FACSCalibur HG Flow Cytometer Instrument (BD Biosciences) and Cell Quest Pro software version 3.1 (BD Biosciences), and the data were analyzed using FlowJo software version 16 (FlowJo LLC).

Protein extraction and western blotting. Protein extraction and western blotting were performed as previously described (19). In brief, proteins from EC cells (HEC1B, HEC50B, HEC265, Ishikawa, HEC151A and HEC116) were extracted using RIPA Buffer (FUJIFILM Wako Pure Chemical Corporation). Protein quantification was performed using Protein Assay bicinchoninic acid (BCA) kit (Nalacai Tesque Inc.) The samples were incubated with BCA working reagent at 37˚C for 30 min. The absorbance of them were measured at 562 nm using a Synergy LX multimode microplate reader (BioTek Instruments, Inc.). The samples (10 μg) were separated using sodium dodecyl sulfate-polyacrylamide gel electrophoresis [SDS-PAGE; Mini-PROTEAN TGX Precast Protein Gels (Any kD™); Bio-Rad Laboratories, Inc.] and transferred by Trans-Blot Turbo Mini polyvinylidene difluoride (PVDF) Transfer Packs (Bio-Rad Laboratories, Inc.). After blocking process, the membrane was incubated with 5% skim milk as blocking solution at 25˚C for 60 min and incubated with the following primary antibodies at 4˚C overnight and incubated with the following secondary antibodies at 25˚C for 60 min. Proteins were detected by Amersham ECL Select (Cytiva) and ImageQuant LAS 4000 (Cytiva). Rabbit anti-PRMT6 (1:1,000; cat. no. 15395-1-AP; Proteintech Group, Inc.); rabbit anti-H3R2me2a (1:1,000; cat. no. ab175007; Abcam); rabbit anti-Histone H3 (1:1,000, cat. no. ab1791; Abcam), and mouse anti-β-actin (1:6,000; cat. no. A2228; Merck KgaA) were used as the primary antibodies. Anti-mouse immunoglobulin G (IgG) HRP-linked antibody (1:3,000; cat. no. 7076; Cell Signaling Technology, Inc.) and anti-rabbit IgG HRP-linked antibody (1:3,000; cat. no. 7074, Cell Signaling Technology, Inc.) were used as secondary antibodies.

ChIP-seq. The EC cells were harvested with trypsin 24, 36, and 48 h following siRNA transfection. ChIP experiments were performed based on the protocol of Maruyama *et al* (27) with certain modifications regarding cell pellets freezing, and antibody concentration and chromatin amount during immunoprecipitation. In brief, the cell pellets after cross-linking were stored at -80˚C. Chromatin was sonicated and fragmented at 4˚C using the Covaris S220 instrument (Covaris, LLC). Dynabeads Protein G (Thermo Fisher Scientific, Inc.) bound to 2.5 μl of the anti-H3K27ac antibodies (cat. no. 8173; Cell Signaling Technology, Inc.) was added to 50 μg chromatin and

incubated at 4˚C overnight. DNA purification was performed using Agencourt AMPure XP (Beckman Coulter, Inc.) and libraries for ChIP-seq were prepared using ThruPLEX® DNA sequencing (DNA-Seq) kit (Takara Bio, Inc.). All samples were sequenced on NextSeq 550 (Illumina, Inc.) as paired-end reads. Five types of anti-H3R2me2a antibodies used for immunoprecipitation did not work well, and their details were as follows: Anti-histone H3 (asymmetric di methyl R2) antibody (2/25 μg chromatin; cat. no. ab175007; Abcam), anti-dimethyl-histone H3 (Arg2) antibody (10/100 μg chromatin; cat. no. 07-585; MilliporeSigma), histone H3 [Asym-dimethyl Arg2] antibody (10/100 μg chromatin; cat. no. NB21-1002; Novus Biologicals, LLC), histone H3R2 dimethyl asymmetric (H3R2me2a) polyclonal antibody (0.1/50 μg chromatin, 0.5/50 μg chromatin, 2/50 μg chromatin; cat. no. A-3714-050; Epigentek Group Inc.), anti-histone H3 (asymmetric di methyl R2) antibody (0.1/50 μg chromatin, 0.5/50 μg chromatin, 1/50 μg chromatin; cat. no. ab194706; Abcam).

RNA sequencing (RNA-seq). Total RNA was extracted from the EC cells 48 h after siRNA transfection using the RNeasy Mini Kit (Qiagen, Valencia, Inc.). Libraries for RNA-seq were prepared using SMARTer® Stranded Total RNA-Seq Kit v3 Pico Input Mammalian (Takara Bio, Inc.). All samples were sequenced on NextSeq 550 (Illumina, Inc.) as paired-end reads.

ChIP-seq analysis. Low-quality reads with a quality value of <25 for >90% of each base pair were first filtered by a fastq_quality_filter. Filtered row reads were mapped to the human genome (hg)38 by bowtie2 (v.2.4.2; https://bowtie-bio.sourceforge.net/bowtie2/index.shtml). Multi-mapped reads and PCR duplicates were then removed using Picard (v.2.25.3; https://broadinstitute.github.io/picard/). The reads overlapped with the Encyclopedia of DNA Elements (ENCODE) black list (https://www.encodeproject.org/files/ENCFF356LFX/) were filtered out by bedtools (2.30.0; https://github.com/arq5x/bedtools2). Model-based Analysis for ChIP-Seq (MACS)2 (v.2.2.7.1; https://github.com/macs3-project/MACS) was utilized for calling peaks with the '-keep-dup auto' parameter. Hypergeometric Optimization of Motif EnRichment (HOMER) (v.4.10; http://homer.ucsd.edu/homer/motif/) was used for identifying differential peaks between siRNA experiments, and motif enrichment analysis. To obtain differential peaks, the 'makeTagDirectory' was first used for creating tag directories from each Binary Alignment Map (bam) file. Subsequently, peak sets of each experiment were merged using 'mergePeaks'. The parameter 'getDifferentialPeaks' was then used with the '-size given -F 2.0 -P 0.05' option. The H3K27ac peaks were classified into seven patterns: i) The pattern one peak was upregulated in siNC and downregulated in siPRMT6#1 and #2; ii) the pattern two peaks were upregulated in siNC and siPRMT6#1 and downregulated in siPRMT6#2; iii) the pattern three peaks were upregulated in siNC and siPRMT6#2; iv) the pattern four peaks were upregulated in siPRMT6#1 and downregulated in siNC and siPRMT6#2; v) the pattern five peaks were upregulated commonly in siPRMT6 and downregulated in siNC; vi) the pattern six peaks were upregulated only in siPRMT6#2; and vii) the pattern seven peaks were commonly upregulated in all samples. To focus on the effect on H3K27ac by PRMT-KD, the pattern five peaks were analyzed further (Fig. S1). To obtain enriched motifs for differential peaks, the 'findMotifsGenome.pl' parameter was used with the '-size given' option. Gene Ontology (GO) analysis was performed using Genomic Regions Enrichment of Annotations Tool (GREAT) version 4.0.4.

RNA-seq analysis. To generate the expression count matrix, row reads were trimmed to remove adaptor sequences by Skewer (v0.2.2; https://github.com/relipmoc/skewer) and mapped to the hg38 genome by Spliced Transcripts Alignment to a Reference (STAR) (v.2.7.8a; https://github.com/alexdobin/STAR); the mapped reads were then counted by featureCounts (v.2.0.10; https://subread.sourceforge.net/featureCounts.html). Upregulated genes were defined as those satisfying the following requirements: i) $\log_2$ fold change >1 and =1; and ii) $\log_2$ average expression >1 and =1. Downregulated genes were defined as those satisfying (1) $\log_2$ fold change <-1 and =1, and (2) $\log_2$ average expression <1 and =1. Gene expression differences between control and siPRMT6 experiments were visualized based on MA plot; genes with (1) $\log_2$ fold change >1 and = 1 (upregulated) or <-1 and =1 (downregulated), and (2) $\log_2$ average expression >1 were identified as differential genes. GO analysis was performed on these genes using the Database for Annotation, Visualization and Integrated Discovery (DAVID) 6.8. The target gene sets of nuclear factor of activated T-cells 1 (NFATC1), SMAD2 and SMAD3 were obtained from ChIP Enrichment Analysis (ChEA) Transcription Factor Targets (SMAD2, SMAD3) and ENCODE Transcript Factor Targets (NFATC1) via Harmonizome 3.0 (https://maayanlab.cloud/Harmonizome/).

Statistical analyses. Statistical analyses were conducted as previously described (19). Comparisons of two groups were performed using unpaired Student's t-test, and comparisons of three groups were performed using one-way analysis of variance (ANOVA) followed by Tukey's post hoc test. The data were analyzed using Excel version 16 (Microsoft Corporation) and John's Macintosh Project (JMP) Pro software version 16 (SAS Institute, Inc.). Kaplan-Meier survival analysis (with the log-rank test) of PRMT6 expression in IHC was analyzed using JMP Pro software version 16 (SAS Institute, Inc.). $P<0.05$ was considered to indicate a statistically significant difference. Each experiment was performed at least in triplicate, and the data are presented as the mean ± standard deviation (SD).

Results

PRMT6 overexpression results in a poor prognosis in EC. In order to examine whether PRMT6 may be an appropriate therapeutic target in EC, the expression of *PRMT6* in EC tissue (n=52, Table SI; patients No. 1 to No. 52) and normal endometrial tissue (n=4; Table SI; N1 to N4 and N17 to N20) was first investigated using RT-qPCR (Figs. 1A and B, and S2). Since there was a statistically significant difference, PRMT6 was significantly overexpressed in EC compared to normal endometrial tissues. Secondly, IHC staining for PRMT6 was performed using clinical specimens of EC (n=55; Table SI; No. 1 to No. 55) and normal endometrial tissue (n=12; Table SI; N5 to N16). PRMT6 expression using IHC was scored by

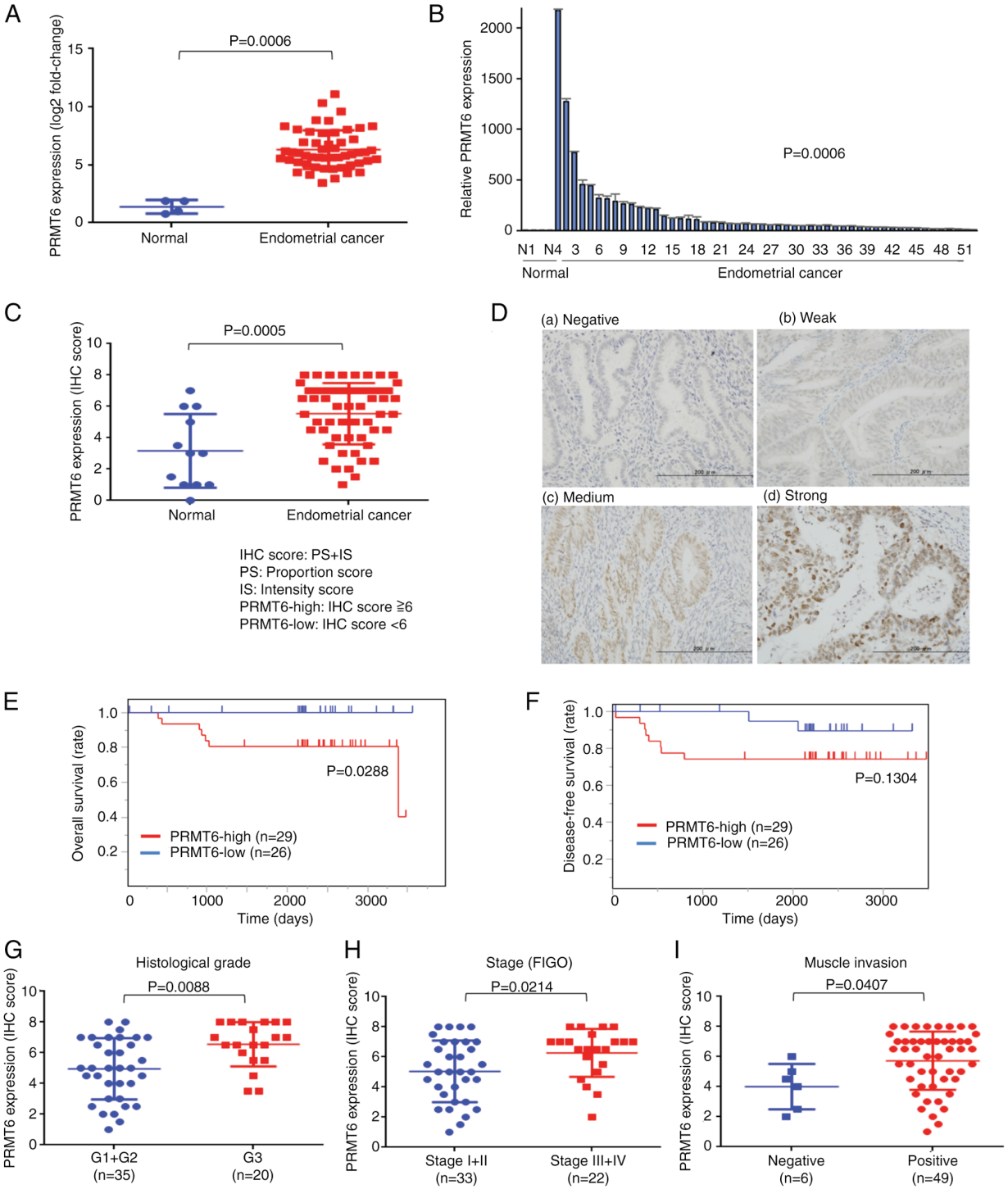

Figure 1. PRMT6 is overexpressed in endometrial cancer and a high expression level is related to a poor prognosis. (A and B) mRNA expression of *PRMT6*. The results of RT-qPCR using clinical specimens of EC (n=52) and normal endometrial tissue (n=4) are presented. (C) The IHC score of PRMT6. The results of IHC using clinical specimens of EC (n=55) and normal endometrial tissue (n=12) are presented. Total score (TS)=proportion score (PS)+intensity score (IS). (D) The staining intensity of PRMT6 by IHC is shown. (a) Normal endometrial tissue, (b-d) EC tissue. IS score 0, background (negative); score 1, weak staining; score 2, moderate staining; score 3, strong staining. Two groups are defined using median as follows: Specimens with scores 0-5 are considered PRMT6-low group and with 6-8 are considered as the PRMT6-high group. The analysis of the OS (E) and DFS (F) in two groups using the Kaplan-Meier method and the log-rank test are presented. The expression of PRMT6 was evaluated using the IHC score (TS) for (G) histological grade, (H) clinical FIGO stage, and (I) muscle invasion. PRMT6, protein arginine methyltransferase 6; RT-qPCR, reverse transcription-quantitative polymerase chain reaction; IHC, immunohistochemistry; EC, endometrial cancer; TS, total score; PS, proportion score; IS, intensity score; OS, overall survival; DFS, disease-free survival; FIGO, The International Federation of Gynecology and Obstetrics.

the PS + IS sum [Fig. 1C and D(a)-D(d)] and was detected to be increased in EC [Fig. 1C and D(b)-D(d)] in comparison with the normal endometrial tissue [Fig. 1C and D(a)]. To assess the clinical significance of PRMT6 in EC, the overall survival (OS) and disease-free survival (DFS) of patients with a high and low expression of PRMT6 was analyzed. OS was

significantly shorter in the PRMT6 high expression group (Fig. 1E). There was no significant difference in DFS; however, a trend towards a shorter DFS was observed in the PRMT6 high expression group (Fig. 1F). Finally, the histopathological classification using PRMT6 expression of the IHC score was evaluated. PRMT6 expression was significantly higher in G3 tissues for the histological grade, stage III and IV according to The International Federation of Gynecology and Obstetrics (FIGO), than in G1 and G2, positive for muscle invasion, FIGO stage I and II and negative for deep muscle invasion stage III/IV (Fig. 1G-I). These data demonstrated that PRMT6 is overexpressed in EC and that high PRMT6 expression levels affect EC progression, resulting in a poor prognosis.

PRMT6 inhibition suppresses EC cell proliferation accompanied by apoptosis with the hypomethylation of H3R2me2a in EC cell lines. In the present study, mainly HEC1B and HEC50B were selected, since these cells are fast-growing and difficult to de-attach from the cell culture dish, rendering cell passaging less demanding. To elucidate the antitumor effects of PRMT6 inhibition in EC cells, PRMT6-KD EC cell lines (HEC1B and HEC50B) were first established using siNC and two types of siPRMT6 (siPRMT6#1 and siPRMT6#2). Subsequently, PRMT6 expression was evaluated using RT-qPCR and western blotting and it was confirmed that PRMT6 expression was suppressed at the mRNA and protein level (Figs. 2A and B, and S3). The H3R2me2a expression levels, catalyzed by PRMT6, were also attenuated by PRMT6-KD (Fig. 2B). Subsequently, cell viability assays were performed, by using six types of PRMT6-KD EC cell lines. Cell viability was suppressed in all six cell lines (Fig. 2C). Finally, the apoptosis levels were evaluated in PRMT6-KD cells using cell cycle analyses and flow cytometry assays. The proportion of cells in the subG1 phase was increased in cell cycle analysis and the proportion of Annexin-positive cells was also increased in the Annexin assay due to PRMT6-KD (Fig. 2D and E). The results of flow cytometry revealed that PRMT6-KD induced the apoptosis of EC cell lines. Hence, these data indicated that PRMT6-KD attenuated the methylation of H3R2me2a and EC cell growth was suppressed with apoptosis.

PRMT6 inhibition induces apoptosis via interferon signaling through H3K27ac in EC cell lines. ChIP assays with H3R2me2a were first performed, in order to clarify the mechanisms through which H3R2me2a, catalyzed by PRMT6, is involved in the suppression of cell proliferation and induction of apoptosis in EC cell lines. A total of five types of commercially available anti-H3R2me2a antibodies were used and the appropriate ChIP protocols were thoroughly considered; however, all the antibodies did not perform adequately. Thus, ChIP experiments with H3K27ac were conducted, which is an active histone mark, to investigate the role of PRMT6 in histone modification using HEC1B. As a preliminary experiment, it was confirmed that PRMT6 was downregulated at the protein level 24 h following transfection with siPRMT6 using western blotting (Fig. S4). Thus, H3K27ac ChIP-seq was performed at three time points, 24, 36 and 48 h, following PRMT6-KD.

In the analysis of H3K27ac ChIP-seq, the analysis was focused on the peak pattern of the signals of H3K27ac enhanced by PRMT6-KD, pattern 5, since H3K27ac is an active histone marker (Fig. S1). The numbers of H3K27ac peaks enhanced in common with two siPRMT6 types were 820, 1,708 and 2,562 peaks, at the time points 24, 36 and 48 h following PRMT6-KD, respectively (Fig. 3A; log2 FC >1 and P-value <0.01). PRMT6 inhibition increased the number of genomic regions in which H3K27ac signals were enhanced over time.

GO analysis of these peak sets with GREAT revealed that interferon-related GO terms were enriched 24 h after PRMT6-KD, apoptosis-related GO terms at 36 h, and cell death-related GO terms at 48 h (Fig. 3B; top 10 enriched terms are shown, FDR <0.01). These results suggested that PRMT6-KD may activate interferon signaling, leading to apoptosis and cell death. It was also observed that interferon-related transcription factor motifs were enriched at all three time points following PRMT6-KD by motif analysis using these peak sets (q-value<0.05) (Fig. 4A). The findings of the present study indicated that PRMT6 inhibition may regulate the genomic regions related to interferon, apoptosis, and cell death via H3K27ac signals.

PRMT6 regulates several interferon and cancer-related transcription factors via H3K27ac in EC cell lines. In order to evaluate the transcription factors that PRMT6 regulates via H3K27ac in EC cell lines, motif analysis using the peak sets presented in Fig. 3A were performed and the motifs were categorized into five groups (Fig. 4A). Group 1 included transcription factor motifs significantly enriched in all three time points peak sets after PRMT6-KD (q-value <0.05). Groups 2, 3 and 4 were transcription factor motifs significantly enriched at each time point 24, 36 and 48 h peak sets after PRMT6-KD, respectively (q-value <0.05). Group 5 included transcription factor motifs significantly enriched in the two time point peak sets, 36 and 48 h following PRMT6-KD (q-value <0.05).

It was considered that groups 1 and 2 included key transcription factor motifs, since they were the first to change triggered by PRMT6-KD. Thus, interferon-related transcription factor motifs and PR/set domain 1 (PRDM1) were identified in group 1 and three transcription factor motifs in group 2, namely NFAT, EBF transcription factor 2 (EBF2) and Tbox:Smad (Fig. 4B). NFAT and EBF2 each consist of the transcription factors NFATC1 and EBF2. Tbox:Smad consists of nodal growth differentiation factor (NODAL), SMAD2, SMAD3 and SMAD4, which are members of the transforming growth factor β (TGF-β) protein group, reported to be related to cancer (28). The changes in the mRNA expression of these transcription factors corresponding to the aforementioned motifs, *PRDM1*, *NFATC1*, *EBF2*, *NODAL*, *SMAD2*, *SMAD3* and *SMAD4*, were evaluated. The transcription factors that presented with altered mRNA expression levels were *NFATC1*, *SMAD2* and *SMAD3*. No significant changes were observed in the expression levels of the other transcription factors (Fig. 4B). Motif analysis indicated that PRMT6 regulated several interferon and cancer-related transcription factors via H3K27ac in EC cell lines.

PRMT6 inhibition alters the expression of 940 genes and increases the expression of interferon-related gene clusters in EC cell lines. In order to identify key downstream genes regulated by PRMT6 in EC cells, RNA-seq was performed. The expression levels of 940 genes were altered

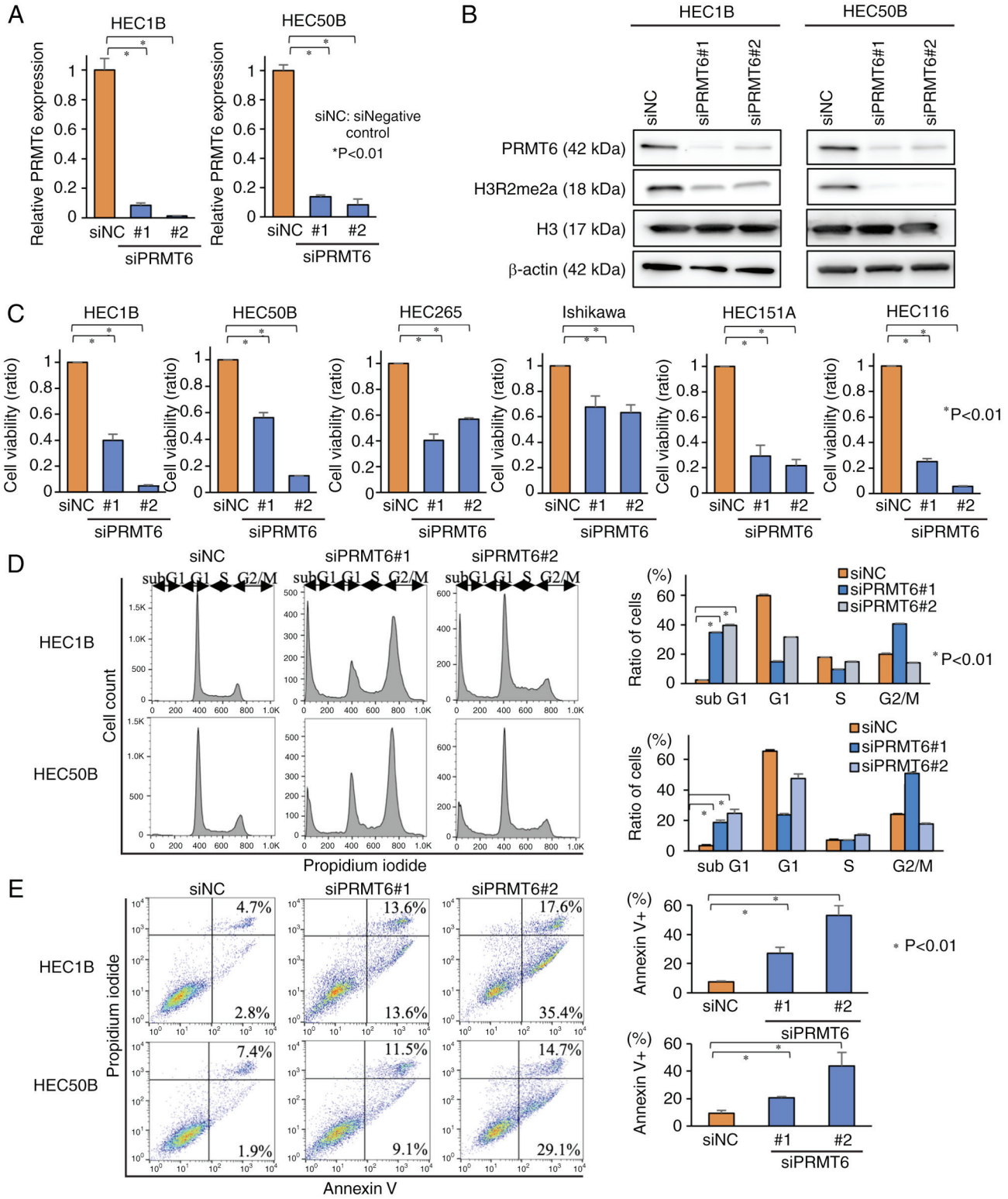

Figure 2. PRMT6 inhibition suppresses EC cell proliferation accompanied by apoptosis with hypomethylation of H3R2me2a. (A) The mRNA expression levels of *PRMT6* evaluated by using RT-qPCR in PRMT6-knockdown EC cell lines (HEC1B and HEC50B) are presented. (B) The protein expression levels of PRMT6 and H3R2me2a evaluated using western blotting in the same cell lines as in (A). (C) Cell viability assay in six types of EC cell lines (HEC1B, HEC50B, HEC265, Ishikawa, HEC151A, and HEC116). Cell cycle analysis (D) and Annexin assay (E) by flow cytometry in PRMT6-knockdown EC cell lines (HEC1B and HEC50B). PRMT6, protein arginine methyltransferase 6; RT-qPCR, reverse transcription-quantitative polymerase chain reaction; H3R2me2a, histone H3R2 dimethylation. P<0.05 was considered to indicate a statistically significant difference. *P<0.01.

48 h following PRMT6-KD (Fig. 5A and B). Furthermore, 423 genes were upregulated and 517 genes were downregulated in common, among the two siPRMT6 datasets (Fig. 5B). Firstly, GO analysis among the 423 upregulated genes was performed using DAVID, to investigate the function of genes whose expression was altered by PRMT6-KD (Fig. 5C and D). Interferon-related and apoptosis-related GO terms which were enriched were identified (P<0.05; Fig. 5D).

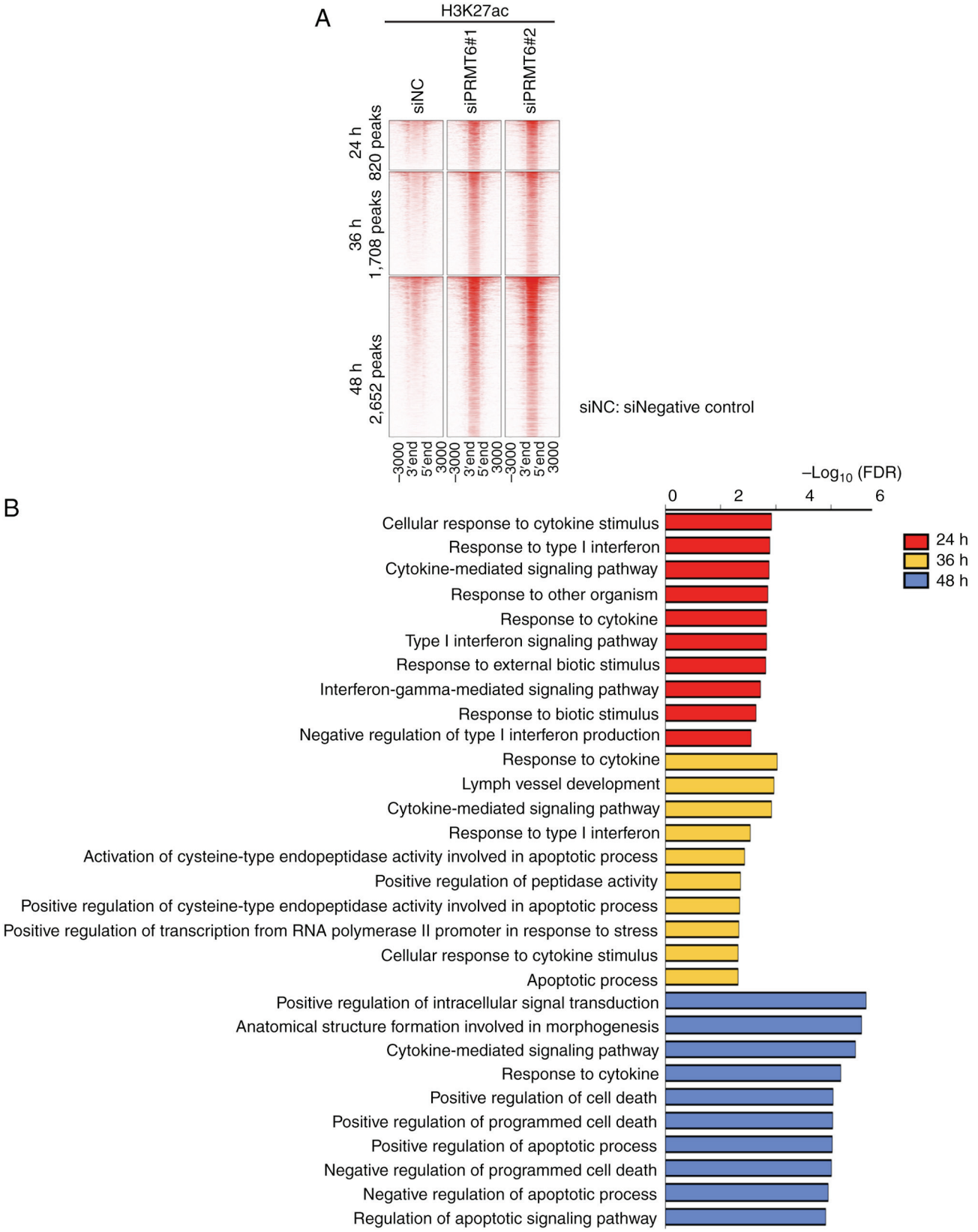

Figure 3. PRMT6 inhibition enhances H3K27ac signals in genomic regions associated with response to interferon, apoptosis, and cell death. (A) Heatmap of H3K27ac ChIP-seq signals significantly enhanced by two siPRMT6s in EC cell line HEC1B (peak center +/- 3 kb). (B) The top 10 biological processes of GO analysis using the peak set presented in (A). PRMT6, protein arginine methyltransferase 6; H3K27ac, histone H3K27 acetylation; ChIP-seq, chromatin immunoprecipitation sequencing; EC, endometrial cancer; GO, Gene Ontology.

These data were consistent with the results of the GO analysis of ChIP-seq. The findings of the present study suggested that PRMT6 inhibition upregulated interferon-related and apoptosis-related genes.

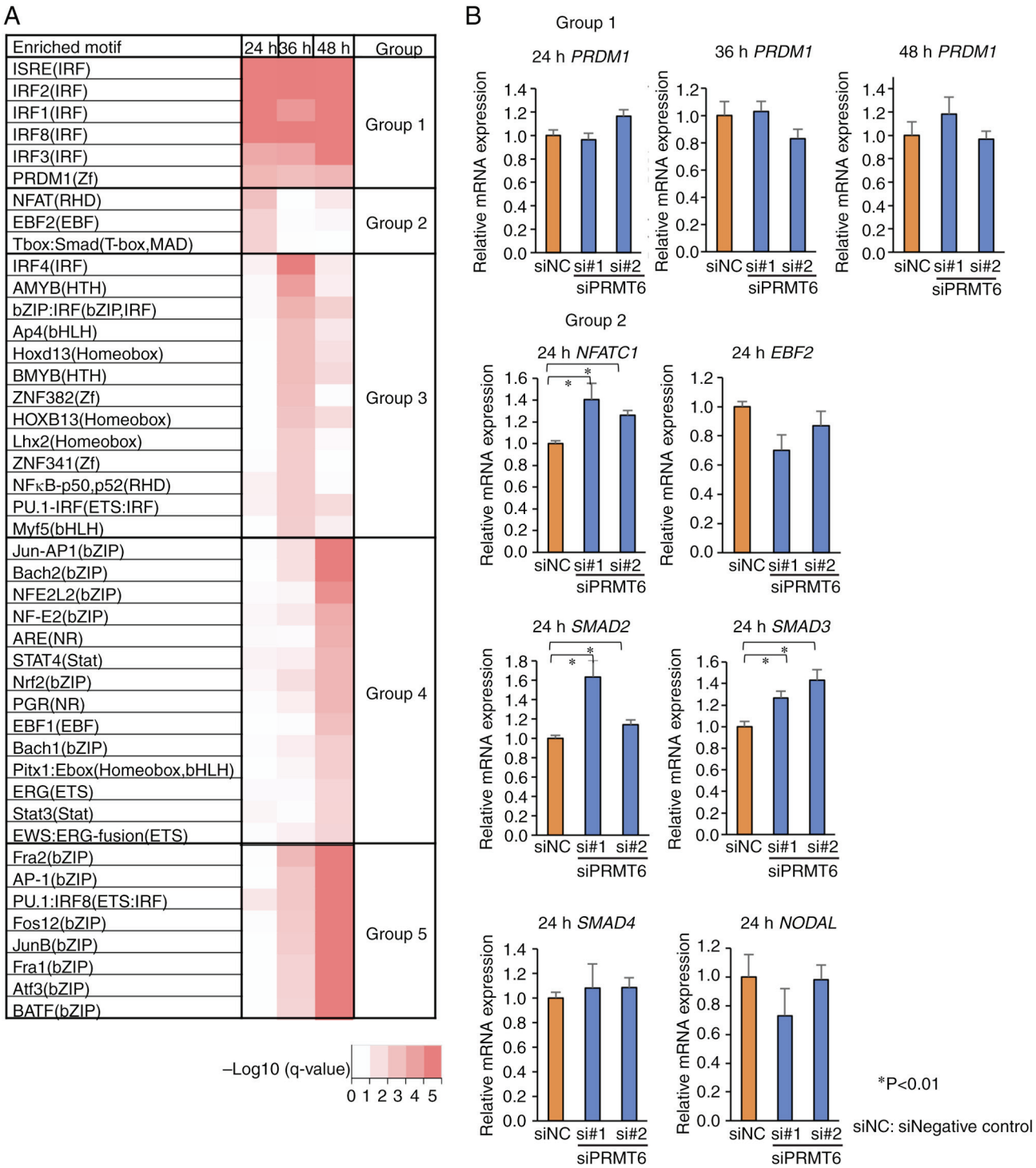

Figure 4. PRMT6 regulates several interferon and cancer-related transcription factors via H3K27ac in EC cell lines. (A) The heatmap of the transcription factor motifs (q-value <0.05) enriched by motif analysis using the peak set previously demonstrated in Fig. 3A. (B) mRNA expression levels of the key transcription factors selected from (A) using RT-qPCR using PRMT6-knockdown EC cell lines. P<0.05 was considered to indicate a statistically significant difference. *P<0.01. PRMT6, protein arginine methyltransferase 6; H3K27ac, histone H3K27 acetylation; RT-qPCR, reverse transcription-quantitative polymerase chain reaction; EC, endometrial cancer; NFAT, nuclear factor of activated T-cells.

Two tumor suppressor genes, NK6 homeobox 1 (NKX6-1) and phosphoinositide-3-kinase regulatory subunit 1 (PIK3R1), are upregulated following PRMT6 inhibition in EC cell lines. In order to identify key downstream genes regulated by PRMT6, the number of genes was curtailed according to the methodology presented in Fig. 5C. The GO terms enriched in the genes whose expression level was increased in common in the two types of siPRMT6 datasets (P<0.05), and GO terms related to cancer and epigenetic regulation were first selected. Each gene function was then considered using PubMed (Fig. 5C) and two key genes were ultimately identified: NKX6-1, a tumor suppressor gene (29-31), and *PIK3R1*, also reported to be related to EC (32). The expression levels of *NKX6-1* and *PIK3R1* were

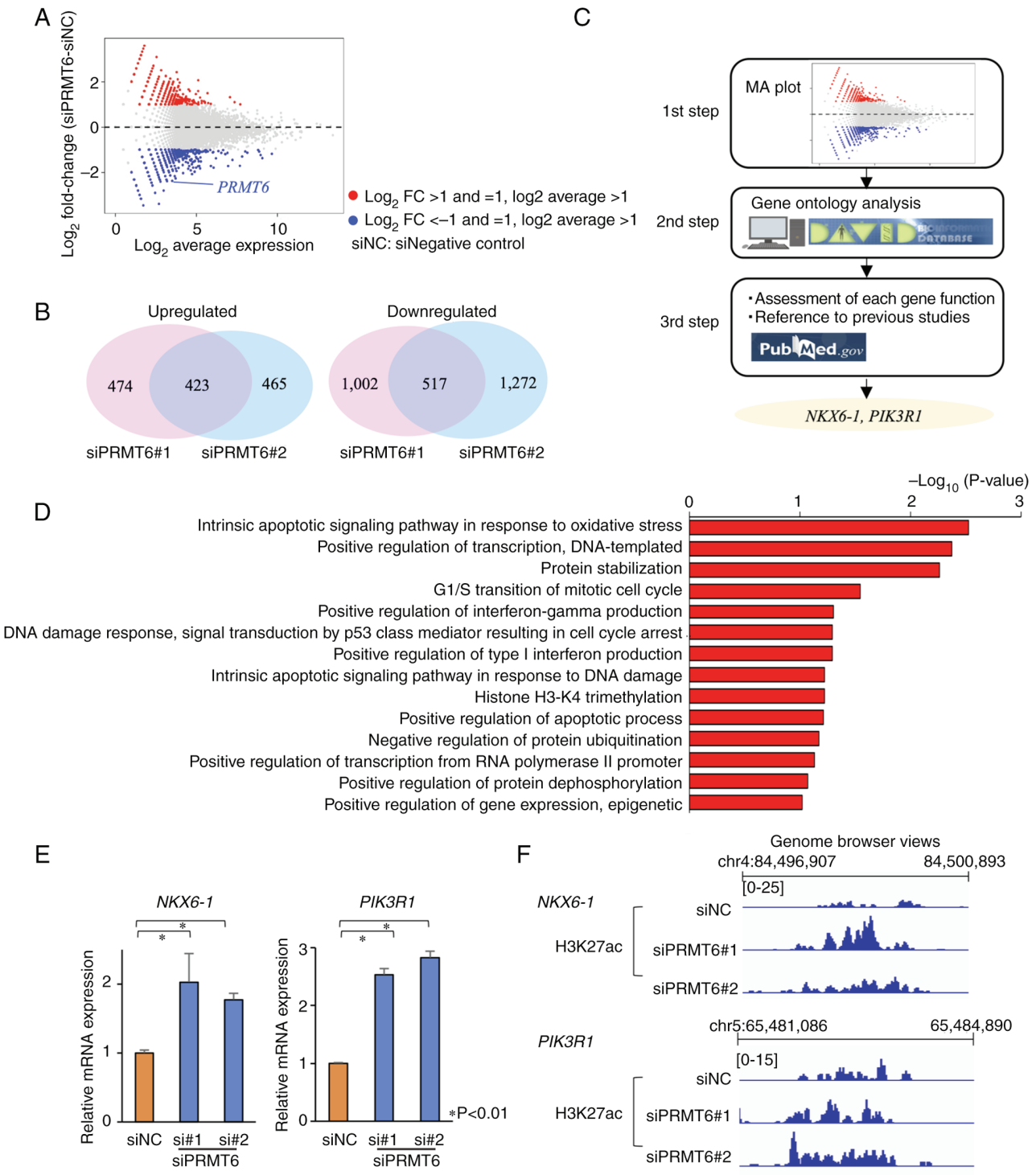

Figure 5. RNA-seq reveals that PRMT6 inhibition alters the expression of 940 genes and increases the expression levels of interferon-related gene clusters in EC cell lines. RNA-seq 48 h after PRMT6-knockdown EC cell line HEC1B. (A) Altered gene expression levels in PRMT6-knockdown EC cells are represented as MA-plot. Red dots, $\log_2$ fold change >1 and = 1, and log2 average expression >1; blue dots, $\log_2$ fold change <-1 and =-1, and log2 average expression >1. (B) The number of upregulated and downregulated genes due to PRMT6-knockdown are shown in the Venn diagram. (C) Flowchart as a method of identifying important genes using RNA-seq data. (D) Biological process of Gene Ontology analysis using the dataset of upregulated genes by PRMT6 knockdown. (E) The mRNA expression levels of *NKX6-1* and *PIK3R1* were evaluated using reverse transcription-quantitative polymerase chain reaction 48 h after PRMT6-knockdown EC cell line HEC1B. (F) The H3K27ac ChIP-seq data 36 h after PRMT6-knockdown EC cell line HEC1B visualized and shown using UCSC genome browser. P<0.05 was considered to indicate a statistically significant difference. *P<0.01. RNA-seq; RNA sequencing; PRMT6, protein arginine methyltransferase 6; EC, endometrial cancer; NKX6-1, NK6 Homeobox 1; PIK3R1, phosphoinositide-3-Kinase Regulatory Subunit 1; ChIP-seq, chromatin immunoprecipitation sequencing.

significantly increased according to the results RT-qPCR (Fig. 5E) and the H3K27ac signals in the two genes were also enhanced according to H3K27 ChIP-seq (Fig. 5F), using PRMT6-KD EC cell lines. The data suggested that PRMT6 inhibition upregulated two tumor suppressor genes, *NKX6-1* and *PIK3R1*.

The expression of *NKX6-1* and *PIK3R1* was also investigated in EC tissues (n=10; Table SI) and normal endometrial tissues (n=4; Table SI), using RT-qPCR (Fig. S5). No significant changes were observed between the EC and normal endometrial tissues.

Interferon-related and apoptosis-related genes are identified downstream of the three transcription factor motifs, NFATC1, SMAD2 and SMAD3. In order to identify interferon and apoptosis-related genes regulated by the three transcription motifs, NFATC1, SMAD2 and SMAD3, as identified using H3K27ac ChIP-seq, an integrated ChIP-seq and RNA-seq analysis was performed. The overlaps of 423 genes upregulated by PRMT6-KD and genes expressing downstream targets of NFATC1, SMAD2 and SMAD3 were evaluated. Among the 423 genes upregulated by PRMT6-KD, the numbers of genes which expressed downstream targets of NFATC1, SMAD2 and SMAD3 were 178, 39 and 63 genes, respectively (Fig. S6). According to GO analysis with the inclusion of those 178, 39, and 63 genes, three interferon-related genes were identified among NFATC1 downstream genes: Interferon regulatory factor 3 (*IRF3*), interferon-stimulated gene 15 (*ISG15*) ubiquitin like modifier (*ISG15*) and interferon regulatory factor 5 (*IRF5*). It was also revealed that multiple apoptosis-related genes exist among the genes expressing targets downstream of NFATC1, SMAD2 and SMAD3 (Figs. S6-S9).

This integrated analysis confirmed that PRMT6-KD may regulate NFATC1, SMAD2 and SMAD3 transcription factors through H3K27ac, and that they regulate in turn multiple interferon and apoptosis-related genes.

PRMT6 inhibition induces the activation of ERV genes in EC cell lines. Recent studies have reported that ERV, whose activation is normally suppressed in humans, is activated by the epigenome and induces interferon secretion in various types of cancer, including multiple myeloma and colorectal cancer (33,34). Therefore, herein, it was evaluated whether PRMT6 inhibition also induces ERV gene activation in EC cell lines. Similar to the ChIP-seq experiments, ERV expression was investigated at the three time points: 24, 36 and 48 h following PRMT6-KD. The expression levels of several ERV genes were significantly increased in the PRMT6-KD EC cells (Fig. 6A) and the expression levels in the majority of the ERV genes were increased 24 h following PRMT6-KD (Fig. 6A and B). Interferon signaling was also induced 24 h after PRMT6-KD by H3K27ac ChIP-seq (Fig. 3B). On the whole, these data indicated that PRMT6-KD may activate ERV genes and induce interferon signaling (Fig. 7).

Finally, the expression of ERV genes in EC tissues (n=10; Table SI) and normal endometrial tissues (n=4, Table SI) were also evaluated using RT-qPCR (Fig. S10). There were no significant differences in ERV gene expression levels between the EC and normal endometrial tissues.

Discussion

The present study investigated whether PRMT6 could be designated as a therapeutic target for the treatment of EC. The increased expression of PRMT6 was observed in clinical samples of EC. KD of PRMT6 inhibited cell proliferation by inducing the apoptosis of EC cell lines. Data from ChIP-seq and RNA-seq also suggested that interferon and apoptotic pathways were activated in PRMT6-KD EC cell lines. In addition, the activation of ERV was identified as a cause of the interferon pathway activation.

PRMT6 has been reported to be highly expressed in a variety of cancer types, including prostate, lung cancer and EC (21,22,24). For example, in a previous study, IHC using colorectal cancer clinical specimens demonstrated a negative association between PRMT6 expression and DFS (35). In another study on gastric cancer, it was demonstrated that both were DFS and OS negatively associated with the expression of PRMT (36). Jiang *et al* (24) performed RT-qPCR and IHC analysis, revealing increased PRMT6 expression in EC compared with normal endometrium. That study also demonstrated, by using The Cancer Genome Atlas database, that the expression of was PRMT6 positively associated with the EC grade or the existence of a special tissue type, including serous carcinoma. Additionally, the expression of PRMT6 was negatively associated with OS (24). In the present study, RT-qPCR, IHC and PRMT6 expression analyses were performed, using clinical specimens of EC at the University of Tokyo Hospital. In comparison with the normal endometrium, an increased PRMT6 expression was observed in EC as previously reported (24), demonstrating a positive association between PRMT6 expression and the pathological grade of EC. The association between PRMT6 expression and prognosis was identical to that of a previous report concerning OS. However, there was no significant difference in DFS. A significant difference in DFS could have been observed if the number of patients was larger. In addition, the present study demonstrated an association between PRMT6 expression, and stage and deep muscle invasion.

KD experiments were also performed, in order to investigate whether PRMT6 is a potential therapeutic target in EC and to examine the antitumor mechanism of PRMT6 suppression. Apoptosis-induced suppression of cell proliferation was observed in EC cells under PRMT6-KD. The suppression of cell proliferation by the inhibition of PRMT6 has been previously reported (37,38). There are some reports on the mechanism of inhibition of cell proliferation by PRMT6. For example, Kleinschmidt *et al* (38) revealed that the KD of PRMT6 inhibits the cell cycle by activating p21. PRMT6 has been reported to enhance the phosphoinositide 3-kinase (PI3K)/AKT/mammalian target of rapamycin (mTOR) pathway as an anti-apoptotic mechanism in prostate cancer (21). It has also been reported that PRMT6 promotes cell proliferation through PI3K/AKT/mTOR pathway in EC (24). However, the effect of PRMT6 on histone modification in EC had not been reported previously, at least to the best of our knowledge. The histone modification of PRMT6 has been reported to asymmetrically dimethylate H3R2 and that H3K27ac and H3K4me3 are affected through methylation of H3R2me2a (23). ChIP-seq analysis using H3R2me2a antibodies is rarely mentioned in the literature and has been solely reported previously by Bouchard *et al* (23), to the best of our knowledge. Initially, ChIP-seq was also performed using H3R2me2a antibodies, without any success (data not shown). This is due to the fact that the ChIP-seq method is a delicate technique influenced by antibodies and the type of cell line, among other factors. Therefore, ChIP-seq for H3K27ac was also performed, which is affected by H3R2me2a.

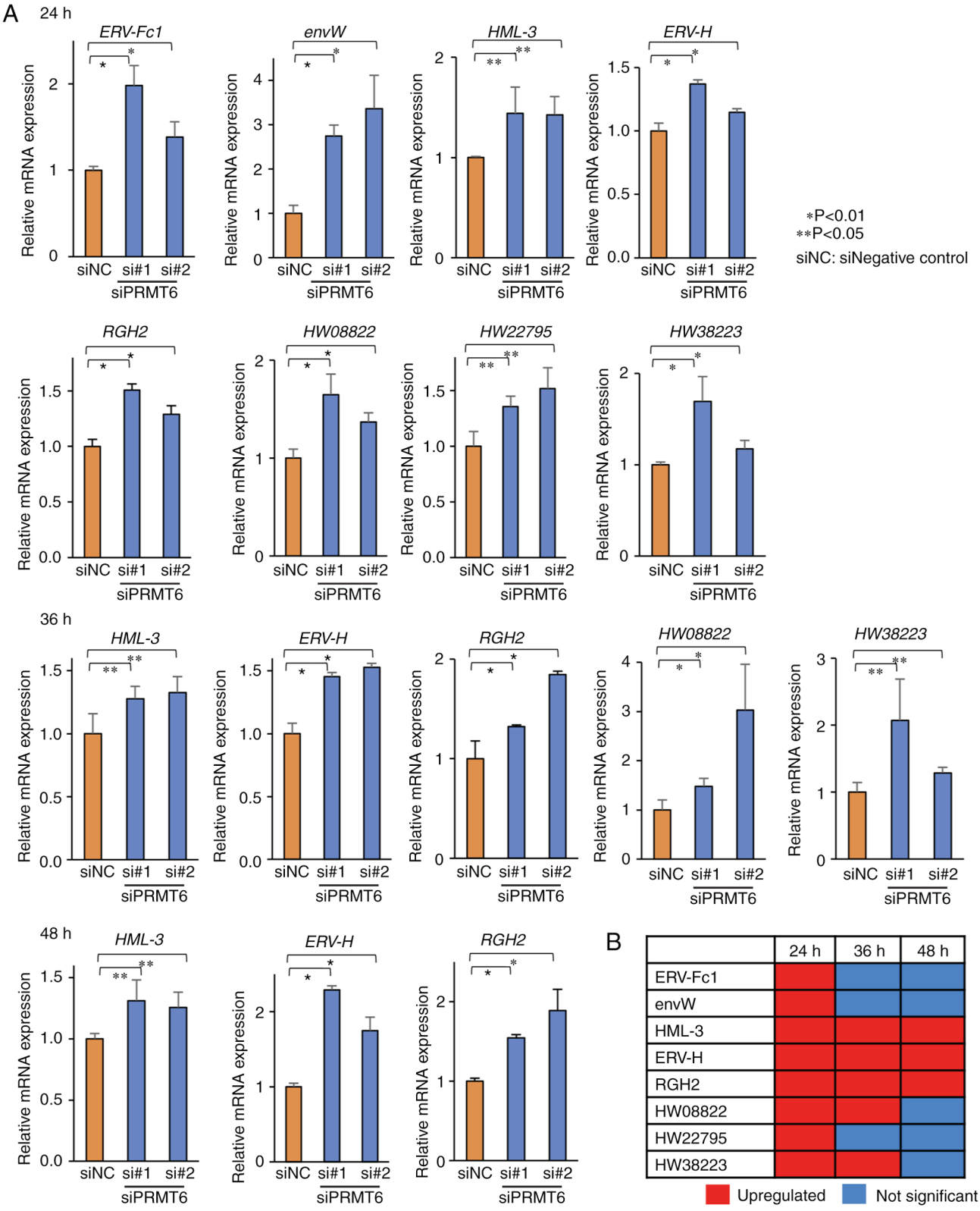

Figure 6. PRMT6 inhibition induces the activation of ERV genes in EC cell lines. (A) mRNA expression levels of ERV evaluated using reverse transcription-quantitative polymerase chain reaction at the three time points: 24, 36, and 48 h after PRMT6 knockdown. (B) The heatmap shows the mRNA expression levels of ERV genes in PRMT6-knockdown EC cell line. P<0.05 was considered to indicate a statistically significant difference. **P<0.05 and *P<0.01. PRMT6, protein arginine methyltransferase 6; ERV, endogenous retrovirus; EC, endometrial cancer.

The KD of PRMT6 demonstrated an increase or decrease in a number of peak patterns of H3K27ac and the present study focused on the increased peak patterns. The time course of H3K27ac was analyzed, using the ChIP-seq method on an hourly basis. The acquired data suggested that histone acetylation, which controls interferon-related, apoptosis-related, and cell death-related genomic regions, was observed to change dynamically with time. When significant transcription

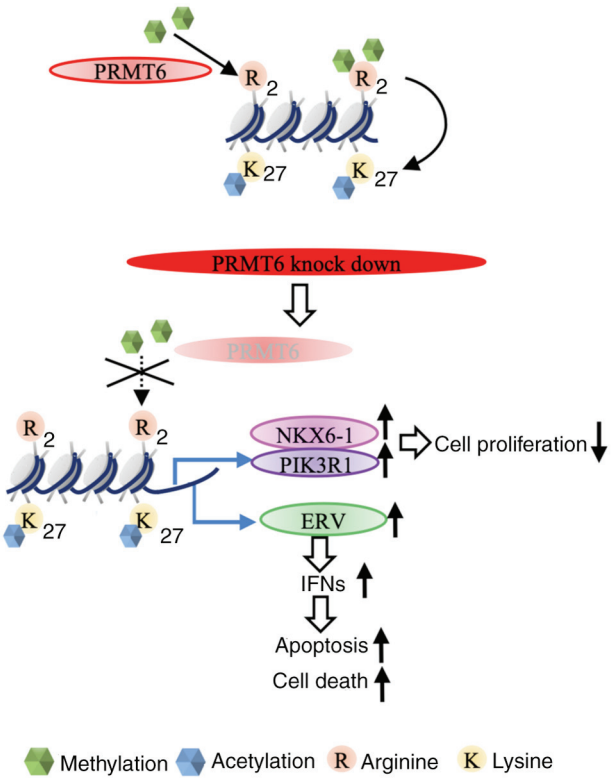

Figure 7. Schematic diagram of antitumor mechanisms through histone modifications in PRMT6 suppression. PRMT6 suppression upregulates two tumor suppressor genes, *NKX6-1* and *PIK3R1*, through histone modification H3K27ac and regulates interferon and apoptosis-related genes. PRMT6 inhibition also activates ERV genes and indicates that ERVs induce interferon signaling. PRMT6, protein arginine methyltransferase 6; NKX6-1, NK6 homeobox 1; PIK3R1, phosphoinositide-3-kinase regulatory subunit 1; H3K27ac, histone H3K27 acetylation; ERV, endogenous retrovirus.

factors regulated by H3K27ac were examined, NFATC1 and SMAD2/3 were identified.

NFAT is a transcription factor that regulates immune system pathways. Among the NFAT family, NFATC1 and NFATC2 are predominantly expressed in T-cells (39). Reppert *et al* (40) reported that NFATC1 promoted interferon-γ. The data of the present study suggested that PRMT6-KD activated interferon signaling and regulated NFATC1. Therefore, these results suggest that NFATC1 is involved in the pathway through which PRMT6-KD promotes the interferon pathway. As was expected, three interferon-related genes and multiple apoptosis-related genes were identified as genes expressing factors downstream of NFATC1, by using integrated analysis of H3K27ac ChIP-seq and upregulated genes by PRMT6-KD in RNA-seq (Figs. S6 and S7).

TGF-β has been identified as a growth factor that promotes cell transformation; however, it also contributes to the inhibition of cell proliferation and the induction of apoptosis in various types of cells, with its physiological effects being diverse (41). Thus, while cell growth suppression has been reported in cancer, the opposite has been reported to induce the epithelial mesenchymal transition (EMT) and promote metastasis (42). In addition, SMAD2/3 is a downstream factor of TGF-β and is important for transmitting TGF-β signaling. Kriseman *et al* (43) suggested that SMAD2/3 is responsible for the normalization of endometrial function and that the absence of SMAD may lead to abnormal cell proliferation and progression in EC. According to the data of the present study, multiple apoptosis-related genes were identified as genes expressing factors downstream of SMAD2 and SMAD3, by using integrated analysis as mentioned above (Figs. S6-S8). Therefore, in view of the results of the present study, an increase in SMAD2/3 levels by PRMT6-KD is suggested as a possible therapeutic mechanism for EC.

Changes in gene expression induced by PRMT6-KD were also analyzed using the RNA-seq method and it was demonstrated that PRMT6-KD altered the expression of various genes. The application of GO analysis and the ChIP-seq method suggested that PRMT6 affected the interferon and apoptotic pathways. In addition, NKX6-1 and PIK3R1 were identified using the RNA-seq method. NKX6-1 is a key transcription factor for pancreatic and neural development and has been reported as a tumor suppressor gene in various types of cancer. For example, it has been reported that NKX6 -1 suppresses the EMT system in cervical and colorectal cancer (29-31). In the present study, the possible involvement of NKX6-1 in EC was reported.

The PI3K/AKT/mTOR pathway is a major signaling pathway required for the maintenance of normal cell functions such as cell proliferation and differentiation. PIK3R1 also acts as a suppressor in the PI3K/AKT/mTOR pathway and a functionally inactive mutation in cancer causes activation of the PI3K/AKT/mTOR pathway (44). Mutations in PIK3R1 are detected in various types of cancer, including EC and colorectal cancer (32). Jiang *et al* (24) also reported that PRMT6 promoted phosphorylation of AKT and activated the PI3K/AKT/mTOR pathway in EC cell lines. A different mechanism was revealed in the present study, demonstrating that PRMT6 reduced PIK3R1 expression level and activated the PI3K/AKT/mTOR pathway by affecting histone modification.

In total, ~10% of mammalian genomes contain sequences derived from ERVs (45). Although regulation of ERVs by epigenome has not been previously reported, some studies have revealed that ERVs, which are normally repressed in humans, are activated by the epigenome, including histone modifications and DNA methylations, to induce interferon (33,34,46,47). For example, Ishiguro *et al* (33) revealed that the inhibition of histone methyltransferase EZH2/G9a stimulated the interferon response by increasing the expression of ERV genes. Similar to previous research (33), the results of the present study demonstrated significant increases in several ERVs by the KD of PRMT6. In the time course of ERV expression, the expression was highest at 24 h after PRMT6-KD, suggesting that ERVs are synchronized with interferon activity. Therefore, the mechanism in which PRMT6-KD stimulates apoptosis by activating interferon via the activation of ERVs is considered.

The expression of ERV genes, *NKX6-1*, and *PIK3R1*, was also examined using RT-qPCR using clinical specimens from endometrial cancer and normal endometrium (Fig. S5). No difference in expression of these genes between EC and the normal endometrium was detected. Since the changes in expression of these genes in the present study may be attributed to PRMT6 suppression, the absence of differences in expression between endometrial carcinoma and normal endometrium is coherent.

The present study has several limitations. Firstly, the ChIP-seq method using the antibody of H3R2me2a methylated by PRMT6 could not be established. Therefore, it is difficult to prove that PRMT6 directly regulates the ERV genes in the present study. Secondly, *in vivo* experiments were not conducted. Several PRMT6 inhibitors are in development at present; however, none of the available inhibitors exhibited adequate specificity to be used in the present study. Mouse experiments will be considered when a prospective PRMT6 selective inhibitor is developed in the future.

In the present study, it was revealed that PRMT6 may be a therapeutic target in EC by affecting multiple genes through changes in histone modifications through the inhibition of PRMT6. Novel tumor suppressor genes, to the best of our knowledge, were also identified, including PIK3R1, transcription factors related to interferon, and ERVs activation by PRMT6-KD through histone modification.

Acknowledgements

Not applicable.

Funding

The present study was supported by the Grant-in-Aid for Scientific Research (B) (Grant no. 20H03820) from the Ministry of Education, Culture, Sports, Science and Technology of Japan.

Availability of data and materials

Sequencing data generated in the present study are available at the Gene Expression Omnibus (GEO) repository (grant no. GSE239296). The other datasets used and/or analyzed during the current study are available from the corresponding author on reasonable request.

Authors' contributions

FI, KS, KKu and RM conceived and designed the study. FI, KS, KKu and KKa designed the experiments. All experiments were performed by FI, KKu, RH and ES. FI and KKu acquired the data. The data were analyzed and interpreted by ST, NT, KKa, YTo, YTa, AT, YM, MT, TI, MM, OWH, KO, HS, RM and YO. FI, KS, KKu and RM prepared the manuscript and figures. ST, NT, KKa, YTo, YTa, MK, AK, HH, AN, AT, YM, MT, TI, MM, OWH, KO, HS, RM, YO reviewed and revised the manuscript for important intellectual content. MK, AK, HH, AN interpreted the data, and provided technical and material support. FI and KS confirm the authenticity of all the raw data. All authors have read and approved the final manuscript.

Ethics approval and consent to participate

In the present study, all patients provided written informed consent for the use of the tumor specimens for research purposes. The present study was approved by the Human Genome, Gene Analysis Research Ethics Committee of the University of Tokyo (approval no. 683-19).

Patient consent for publication

Not applicable.

Competing interests

KO obtained research grants from Daiichi-Sankyo Co., Ltd. and AstraZeneca plc, as well as lecture fees from Chugai Pharmaceutical Co., Ltd. and AstraZeneca plc. All of the remaining authors declare that they have no competing interests.

References

1. Anderson AS, Key TJ, Norat T, Scoccianti C, Cecchini M, Berrino F, Boutron-Ruault MC, Espina C, Leitzmann M, Powers H, *et al*: European code against cancer 4th edition: Obesity, body fatness and cancer. Cancer Epidemiol 39 (Suppl 1): S34-S45, 2015.
2. Lachance JA, Darus CJ and Rice LW: Surgical management and postoperative treatment of endometrial carcinoma. Rev Obstet Gynecol 1: 97-105, 2008.
3. Makker V, Colombo N, Casado Herráez A, Santin AD, Colomba E, Miller DS, Fujiwara K, Pignata S, Baron-Hay S, Ray-Coquard I, *et al*: Lenvatinib plus pembrolizumab for advanced endometrial cancer. N Engl J Med 386: 437-448, 2022.
4. Hanahan D: Hallmarks of cancer: New dimensions. Cancer Discov 12: 31-46, 2022.
5. Zhang L, Lu Q and Chang C: Epigenetics in health and disease. Adv Exp Med Biol 1253: 3-55, 2020.
6. Margueron R, Trojer P and Reinberg D: The key to development: Interpreting the histone code? Curr Opin Genet Dev 15: 163-176, 2005.
7. Strahl BD and Allis CD: The language of covalent histone modifications. Nature 403: 41-45, 2000.
8. Varier RA and Timmers HT: Histone lysine methylation and demethylation pathways in cancer. Biochim Biophys Acta 1815: 75-89, 2011.
9. Hamamoto R, Saloura V and Nakamura Y: Critical roles of non-histone protein lysine methylation in human tumorigenesis. Nat Rev Cancer 15: 110-124, 2015.
10. Sone K, Piao L, Nakakido M, Ueda K, Jenuwein T, Nakamura Y and Hamamoto R: Critical role of lysine 134 methylation on histone H2AX for γ-H2AX production and DNA repair. Nat Commun 5: 5691, 2014.
11. Oki S, Sone K, Oda K, Hamamoto R, Ikemura M, Maeda D, Takeuchi M, Tanikawa M, Mori-Uchino M, Nagasaka K, *et al*: Oncogenic histone methyltransferase EZH2: A novel prognostic marker with therapeutic potential in endometrial cancer. Oncotarget 8: 40402-40411, 2017.
12. Kojima M, Sone K, Oda K, Hamamoto R, Kaneko S, Oki S, Kukita A, Machino H, Honjoh H, Kawata Y, *et al*: The histone methyltransferase WHSC1 is regulated by EZH2 and is important for ovarian clear cell carcinoma cell proliferation. BMC Cancer 19: 455, 2019.
13. Kukita A, Sone K, Oda K, Hamamoto R, Kaneko S, Komatsu M, Wada M, Honjoh H, Kawata Y, Kojima M, *et al*: Histone methyltransferase SMYD2 selective inhibitor LLY-507 in combination with poly ADP ribose polymerase inhibitor has therapeutic potential against high-grade serous ovarian carcinomas. Biochem Biophys Res Commun 513: 340-346, 2019.
14. Kojima M, Sone K, Oda K, Hamamoto R, Kaneko S, Oki S, Kukita A, Kawata A, Honjoh H, Kawata Y, *et al*: The histone methyltransferase SMYD2 is a novel therapeutic target for the induction of apoptosis in ovarian clear cell carcinoma cells. Oncol Lett 20: 153, 2020.
15. Wada M, Kukita A, Sone K, Hamamoto R, Kaneko S, Komatsu M, Takahashi Y, Inoue F, Kojima M, Honjoh H, *et al*: Epigenetic modifier SETD8 as a therapeutic target for high-grade serous ovarian cancer. Biomolecules 10: 1686, 2020.
16. Blanc RS and Richard S: Arginine methylation: The coming of age. Mol Cell 65: 8-24, 2017.
17. Bedford MT and Clarke SG: Protein arginine methylation in mammals: Who, what, and why. Mol Cell 33: 1-13, 2009.
18. Yang Y and Bedford MT: Protein arginine methyltransferases and cancer. Nat Rev Cancer 13: 37-50, 2013.

19. Inoue F, Sone K, Toyohara Y, Tanimoto S, Takahashi Y, Kusakabe M, Kukita A, Honjoh H, Nishijima A, Taguchi A, *et al*: Histone arginine methyltransferase CARM1 selective inhibitor TP-064 induces apoptosis in endometrial cancer. Biochem Biophys Res Commun 601: 123-128, 2022.
20. Dowhan DH, Harrison MJ, Eriksson NA, Bailey P, Pearen MA, Fuller PJ, Funder JW, Simpson ER, Leedman PJ, Tilley WD, *et al*: Protein arginine methyltransferase 6-dependent gene expression and splicing: Association with breast cancer outcomes. Endocr Relat Cancer 19: 509-526, 2012.
21. Almeida-Rios D, Graça I, Vieira FQ, Ramalho-Carvalho J, Pereira-Silva E, Martins AT, Oliveira J, Gonçalves CS, Costa BM, Henrique R and Jerónimo C: Histone methyltransferase PRMT6 plays an oncogenic role of in prostate cancer. Oncotarget 7: 53018-53028, 2016.
22. Avasarala S, Wu PY, Khan SQ, Yanlin S, Van Scoyk M, Bao J, Di Lorenzo A, David O, Bedford MT, Gupta V, *et al*: PRMT6 promotes lung tumor progression via the alternate activation of tumor-associated macrophages. Mol Cancer Res 18: 166-178, 2020.
23. Bouchard C, Sahu P, Meixner M, Nötzold RR, Rust MB, Kremmer E, Feederle R, Hart-Smith G, Finkernagel F, Bartkuhn M, *et al*: Genomic location of PRMT6-dependent H3R2 methylation is linked to the transcriptional outcome of associated genes. Cell Rep 24: 3339-3352, 2018.
24. Jiang N, Li QL, Pan W, Li J, Zhang MF, Cao T, Su SG and Shen H: PRMT6 promotes endometrial cancer via AKT/mTOR signaling and indicates poor prognosis. Int J Biochem Cell Biol 120: 105681, 2020.
25. Livak KJ and Schmittgen TD: Analysis of relative gene expression data using real-time quantitative PCR and the 2(-Delta Delta C(T)) method. Methods 25: 402-408, 2001.
26. Ohtani H, Liu M, Zhou W, Liang G and Jones PA: Switching roles for DNA and histone methylation depend on evolutionary ages of human endogenous retroviruses. Genome Res 28: 1147-1157, 2018
27. Maruyama R, Choudhury S, Kowalczyk A, Bessarabova M, Beresford-Smith B, Conway T, Kaspi A, Wu Z, Nikolskaya T, Merino VF, *et al*: Epigenetic regulation of cell type-specific expression patterns in the human mammary epithelium. PLoS Genet 7: e1001369, 2011.
28. Kim SW, Yoon SJ, Chuong E, Oyolu C, Wills AE, Gupta R and Baker J: Chromatin and transcriptional signatures for nodal signaling during endoderm formation in hESCs. Dev Biol 357: 492-504, 2011.
29. Chang CC, Huang RL, Wang HC, Liao YP, Yu MH and Lai HC: High methylation rate of LMX1A, NKX6-1, PAX1, PTPRR, SOX1, and ZNF582 genes in cervical adenocarcinoma. Int J Gynecol Cancer 24: 201-209, 2014.
30. Li HJ, Yu PN, Huang KY, Su HY, Hsiao TH, Chang CP, Yu MH and Lin YW: NKX6.1 functions as a metastatic suppressor through epigenetic regulation of the epithelial-mesenchymal transition. Oncogene 35: 2266-2278, 2016.
31. Chung HH, Lee CT, Hu JM, Chou YC, Lin YW and Shih YL: NKX6.1 represses tumorigenesis, metastasis and chemoresistance in colorectal cancer. J Mol Sci 21: 5106, 2020.
32. Cheung LW and Mills GB: Targeting therapeutic liabilities engendered by PIK3R1 mutations for cancer treatment. Pharmacogenomics 17: 297-307, 2016.
33. Ishiguro K, Kitajima H, Niinuma T, Maruyama R, Nishiyama N, Ohtani H, Sudo G, Toyota M, Sasaki H, Yamamoto E, *et al*: Dual EZH2 and G9a inhibition suppresses multiple myeloma cell proliferation by regulating the interferon signal and IRF4-MYC axis. Cell Death Discov 7: 7, 2021.
34. Roulois D, Loo Yau H, Singhania R, Wang Y, Danesh A, Shen SY, Han H, Liang G, Jones PA, Pugh TJ, *et al*: DNA-demethylating agents target colorectal cancer cells by inducing viral mimicry by endogenous transcripts. Cell 162: 961-973, 2015.
35. Lim Y, Yu S, Yun JA, Do IG, Cho L, Kim YH and Kim HC: The prognostic significance of protein arginine methyltransferase 6 expression in colon cancer. Oncotarget 9: 9010-9020, 2018.
36. Okuno K, Akiyama Y, Shimada S, Nakagawa M, Tanioka T, Inokuchi M, Yamaoka S, Kojima K and Tanaka S: Asymmetric dimethylation at histone H3 arginine 2 by PRMT6 in gastric cancer progression. Carcinogenesis 40: 15-26, 2019.
37. Stein C, Riedl S, Rüthnick D, Nötzold RR and Bauer UM: The arginine methyltransferase PRMT6 regulates cell proliferation and senescence through transcriptional repression of tumor suppressor genes. Nucleic Acids Res 40: 9522-9533, 2012.
38. Kleinschmidt MA, de Graaf P, van Teeffelen HA and Timmers HT: Cell cycle regulation by the PRMT6 arginine methyltransferase through repression of cyclin-dependent kinase inhibitors. PLoS One 7: e41446, 2012.
39. Rao A, Luo C and Hogan PG: Transcription factors of the NFAT family: Regulation and function. Annu Rev Immunol 15: 707-747, 1997.
40. Reppert S, Zinser E, Holzinger C, Sandrock L, Koch S and Finotto S: NFATc1 deficiency in T cells protects mice from experimental autoimmune encephalomyelitis. Eur J Immunol 45: 1426-1440, 2015.
41. Zhang Y, Alexander PB and Wang XF: TGF-β family signaling in the control of cell proliferation and survival. Cold Spring Harb Perspect Biol 9: a022145, 2017.
42. Ribatti D, Tamma R and Annese T: Epithelial-mesenchymal transition in cancer: A historical overview. Transl Oncol 13: 100773, 2020.
43. Kriseman M, Monsivais D, Agno J, Masand RP, Creighton CJ and Matzuk MM: Uterine double-conditional inactivation of Smad2 and Smad3 in mice causes endometrial dysregulation, infertility and uterine cancer. Proc Natl Acad Sci USA 116: 3873-3882, 2019.
44. Hennessy BT, Smith DL, Ram PT, Lu Y and Mills GB: Exploiting the PI3K/AKT pathway for cancer drug discovery. Nat Rev Drug Discov 4: 988-1004, 2005.
45. European Bioinformatics Institute; Ewan B, Nick G, Arkadiusz K, Emmanuel M, Alistair RG, Guy S, Arne S, Abel UV, Simon W, *et al*: Initial sequencing and comparative analysis of the mouse genome. Nature 420: 520-562, 2002.
46. Goodier JL: Restricting retrotransposons: A review. Mob DNA 7: 16, 2016.
47. Chiappinelli KB, Strissel PL, Desrichard A, Li H, Henke C, Akman B, Hein A, Rote NS, Cope LM, Snyder A, *et al*: Inhibiting DNA methylation causes an interferon response in cancer via dsRNA including endogenous retroviruses. Cell 169: 361, 2017.